Simulation of I-V curves of small Josephson tunnel junctions with finite capacitance

D. E. Prober
Becton Center, Department of Engineering and Applied Science, Yale University, New Haven, Connecticut 06520

S. E. G. Slusky
Bell Laboratories, Crawford Hill Laboratory, Holmdel, New Jersey 07733

R. W. Henry
Becton Center, Department of Engineering and Applied Science, Yale University, New Haven, Connecticut 06520;
and Physics Department, Bucknell University, Lewisburg, Pennsylvania 17837[a]

L. D. Jackel
Bell Laboratories, Holmdel, New Jersey 07733

(Received 13 October 1980; accepted for publication 16 January 1981)

Results of digital and analog simulations of the I-V characteristics of small Josephson tunnel junctions are presented for a variety of cases, and are compared with the recent experimental results of Howard *et al.* [Appl. Phys. Lett. **35**, 879 (1979)] on small-area, high-current-density junctions. The lumped-circuit-element model of Stewart and McCumber with an adjustable nonlinear quasiparticle conductance and various capacitance values is employed. The value of junction capacitance inferred from the digital simulation for a 10^{-9}-cm^2 junction is 9×10^{-15} F. This represents a normalized capacitance $\beta_c = 0.3$ for the junction considered, which had a critical current density $\approx 10^5$ A/cm^2. The inferred capacitance is in agreement with the value extrapolated from previous experimental results. Both digital and analog simulations result in I-V curves which show a previously unreported crossing of the quasiparticle and total current curves. This crossing is due to an averaging in time of the voltage across the nonlinear quasiparticle-conductance channel. The crossing is not seen in the experimental results of Howard *et al.* Differences between the experimental and simulated I-V curves are discussed.

PACS numbers: 74.50. + r,73.40.Rw

I. INTRODUCTION

In recent years Josephson tunnel junction devices have been of increasing interest in a variety of electronic applications, including sensitive magnetometers and voltmeters, high-frequency detectors, and fast digital computer and signal processing circuits. However, most tunnel junctions suffer from having a large shunt capacitance, which can prevent their use in many of the analog applications. This capacitance also places a lower limit on the RC switching time in digital applications, and results in latching logic circuits which require an ac power supply.

Recently, much effort has been devoted to removing the deficiencies which result from large junction capacitance. Reduction of the junction area, and hence capacitance, has also been achieved, with the use of advanced lithographic techniques. Howard *et al.* have produced ultrasmall junctions[1,2] with areas 10^{-9}–10^{-10} cm^2, in which the effects of shunt capacitance are significantly reduced. The successful fabrication of these junctions allows direct tests of the various theoretical models for the behavior of tunnel junctions with little capacitive shunting.

In this paper we present digital and analog simulations of the I-V curves of such ultrasmall junctions, and compare the results of the simulations to the experimental data.[1] The purpose of this work is to study the applicability for very small junctions of the lumped-circuit-element model which has been employed extensively to explain the behavior of large junctions.[3] As previous simulations of tunnel junction I-V curves[4–6] have been restricted to specific junction parameters, we also present here results from the analog simulations for a wide range of junction parameters, to allow comparison with future experiments.

II. MODEL AND METHODS OF SIMULATION

The simulations to be described use the lumped-circuit-element model of a Josephson oxide-barrier tunnel junction, in which the junction current is given as[3]

$$I = I_c \sin\theta + I_{qp}(V) + C\frac{dV}{dt} \tag{1}$$

and

$$\frac{d\theta}{dt} = \frac{2\pi}{\phi_0} V \tag{2}$$

with θ the quantum phase difference across the junction, I_c the critical current, $I_{qp}(V)$ the voltage-dependent quasiparticle current, C the junction capacitance, and ϕ_0 the superconducting flux quantum $= h/2e = 2.07\times10^{-15}$ V sec. (The quasiparticle conductance G_{qp} is defined as $I_{qp}(V)/V$. With $G_{qp} = R^{-1}$, a constant, Eqs. (1) and (2) describe the resistively shunted junction (RSJ) model of Stewart and McCumber.[8]) The model of Eqs. (1) and (2) is often called the resistively shunted junction model with a nonlinear quasiparticle conductance. For the small junctions to be consid-

[a]Permanent address.

 0021-8979/81/064145-05$01.10

ered here, the phase difference θ is uniform across the junction, because the junction dimensions are $\leqslant \lambda_J$, the Josephson penetration depth.[7]

In the RSJ model the parameter β_c specifies the normalized capacitance. For tunnel junctions we define β_c to be

$$\beta_c = 2\pi I_c R_n^2 C/\phi_0 \tag{3}$$

with $R_n^{-1} \equiv G_n$, the normal-state conductance, which is equal to the quasiparticle conductance at voltages well above the gap voltage V_g. We retain this parameter in our discussion of tunnel junctions because it is a prime determinant of the hysteresis of the tunnel junction I-V curves.

In the discussions which follow, the junction is treated as being current biased, so that in Eq. (1), $I = I_{dc}$, a constant. The external circuitry supplies this dc current. At high voltages, and thus at high frequencies, the series inductive impedance of the film electrodes would also tend to current bias the junction.[9] In the measurements by Howard *et al.*[1] 20-μm-wide strips lead to the junction. We estimate an inductance of about 10 pH per square for these strips, so that in the 500-GHz frequency range, the inductive impedance of a few squares of strip length exceeds the junction impedance.

The series inductive impedance of the electrodes also prevents most of the electrode capacitance from affecting the junction I-V characteristics.[9] We roughly estimate that only the capacitance between the first 20-μm lengths of the electrodes can affect the junction. This capacitance is a few fF (1 fF = 10^{-15} F), and thus will not significantly increase the effective junction capacitance which determines the I-V characteristics. Still, the capacitance value one can infer from the hysteresis in the I-V curves (see below) represents an upper bound on the "intrinsic" junction capacitance.

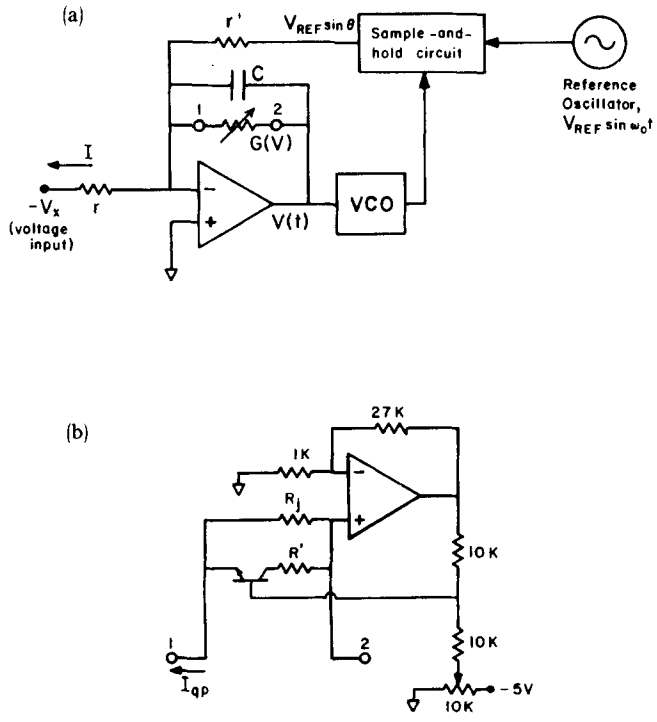

FIG. 1. (a) Circuit of electronic analog. The total "junction" current $I = V_x/r$, is given by Eq. (5). Operational amplifier is a type 741, voltage controlled oscillator (VCO) a type 555. Sample-and-hold circuit is a CMOS 4066 switch, driven by the VCO to sample the sinusoidal reference voltage once each cycle, and followed by a 500-pF storage capacitor and unity-gain 741 buffer; $r' = r = 10\ \text{k}\Omega$. (b) Bipolar transistor switch circuit used as nonlinear quasiparticle conductance, $G(V)$. Voltage of 10-kΩ potentiometer controls V_g, the breakpoint of $G(V)$. $R_n \approx R_j R'/(R_j + R')$. Operational amplifier is a type 741; transistor 2N3642. Voltage at tap on 10 kΩ potentiometer is -3.52 V.

Two different methods of simulation were employed to obtain the results we present. One method involved digital techniques; the other, analog. Digital simulation of current-biased junctions was carried out by solving the second-order differential equation implied by Eqs. (1) and (2). That second-order equation was solved numerically using the improved Euler method.[10]

Junction parameters of the digital simulation were taken from the experimental data. The voltage-dependent conductance $G_{qp}(V)$ for Eq. (1) was derived from the measured quasiparticle I-V curve of the ultrasmall junction of Howard *et al.*[1]. Their quasiparticle curve $I_{qp}(V)$ was measured by applying a magnetic field to suppress I_c to zero. The capacitance C was taken as a variable in the digital simulation.

Analog simulations of current-biased tunnel junctions were carried out with a phase-locked-loop electronic junction analog. Extensive results have been obtained with this analog for the RSJ model and for dc and rf SQUID's.[11] These results agree well with results in the literature, and will be reported elsewhere.

A circuit diagram of the junction analog employed is shown in Fig. 1. In the electronic analog the quantum phase difference is modeled by the phase difference between a voltage-controlled oscillator (VCO) and a fixed-frequency reference oscillator with an angular frequency $\omega_0 \sim 6\times 10^5$ rad/sec. (See Fig. 1.) The instantaneous VCO angular frequency is $d\theta_{VCO}/dt = [2\pi V(t)/\lambda] + \omega_0$, with λ a constant. The VCO produces a pulse for each 2π increase of its phase; these pulses drive a sample-and-hold circuit which samples the *sinusoidal* reference oscillator signal every $\approx 10\,\mu$sec. The smoothed voltage output of the sample-and-hold circuit is thus proportional to the sine of the phase difference θ between the VCO and reference oscillator,

$$\theta \equiv \theta_{VCO} - \theta_{REF} = \int \frac{2\pi}{\lambda} V(t)\,dt, \tag{4}$$

in analogy to Eq. (2).

The operational amplifier in Fig. 1(a) is in the standard inverting configuration. Therefore the virtual ground approximation applies; the negative terminal is at ground potential and the sum of the currents into the negative terminal is zero. As a result, the total applied current $I = V_x/r$ is given by

$$I = \frac{V_{REF}}{r'}\sin\theta + G(V)V + C\frac{dV}{dt}. \tag{5}$$

The electronic circuit is thus an exact analog of the Josephson junction described by Eqs. (1) and (2). The identifications $I_c \rightarrow V_{REF}/r'$ and $G_{qp}(V) \rightarrow G(V)$ apply; λ is the analog of the flux quantum ϕ_0.

The voltage-dependent conductance $G(V)$ is implemented with a bipolar transistor switch, as shown in Fig. 1(b). In this circuit the junction voltage is amplified, and used to close the transistor switch when $V > V_g$. Quasiparticle I-V

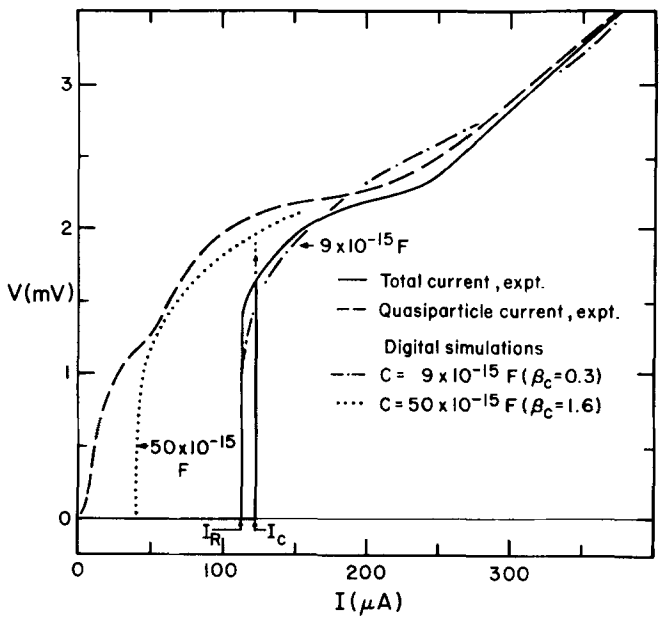

FIG. 2. Current-voltage curves from digital simulations for $C = 9\times10^{-15}$ F and $C = 50\times10^{-15}$ F, and experimental curves (Ref. 1) of the total junction current I and the quasiparticle current. The critical current I_c, and return current, I_R, are noted for the experimental curve. Simulation curve for 9×10^{-15} F has same value of I_R; note that this curve crosses the quasiparticle curve twice. Curve for 50×10^{-15} F is not shown above 150 μA; it exhibits a similar crossing.

curves were approximated by three straight line segments (shown below). β_c and the subgap quasiparticle resistance R_j (for $V < V_g$) were adjustable. V_g/I_cR_n was set to be ~ 1.7, close to that of the experimental data although larger than the zero-temperature theoretical value. The resulting quasiparticle curves are a much better approximation to the characteristics of real junctions than those produced in other electronic analogs.[12]

III. RESULTS

The results of the digital simulation for the time-average junction voltage V as a function of the total junction current I are plotted in Fig. 2. Curves for $C = 9\times10^{-15}$ F and $C = 50\times10^{-15}$ F are shown. The value $C = 9\times10^{-15}$ F gives the best fit to the hysteresis of the experimental total current curve (solid line). This value of C corresponds to $\beta_c = 0.3$.

Results obtained with the analog simulation are presented in Figs. 3(a) and 3(b). In Fig. 3(a), the subgap resistance R_j is equal to $4R_n$; in Fig. 3(b), $R_j = 2R_n$, typical of a junction with significant subgap leakage current. These two values of R_j/R_n were chosen because the subgap conductance of the experimental quasiparticle curve falls between these two limits. Results for various values of β_c appear in Figs. 3(a) and 3(b).

A surprising feature of both the digital and analog simulations of Figs. 2 and 3 is that the average voltage crosses the quasiparticle (dashed) curve twice. Only at high voltages, $V \gg V_g$, does the simulated curve approach the quasiparticle curve. This double crossing is *not* seen for the $H = 0$ experimental data (solid line, Fig. 2). We shall discuss the discrepancy below.

An overall trend of the data in Fig. 3 is that, for fixed β_c, the hysteresis increases with increasing subgap resistance. This is in agreement with the experimental conclusion of Howard *et al.* The curves for $\beta_c = 0.3$ (the value set by the digital results) give $I_R/I_c = 0.87$ and 0.98 for $R_j/R_n = 4$ and 2, respectively. (I_R is the current at which the voltage returns to zero.) These values of I_R/I_c bracket the experimental value of $I_R/I_c = 0.93$.

In Fig. 4 we plot I_R/I_c as a function of β_c. Data from numerous sources are included in this figure. Results from our analog and digital simulations of the RSJ model (constant G_{qp}) are shown. Note how closely these correspond with McCumber's calculation[8] for the RSJ model. Our results from the analog simulations with nonlinear $G_{qp}(V)$ are also shown. The trend of increased hysteresis with increasing R_j is again evident here. We also plot for comparison the results of Stewart[5] who computed I-V curves for quasiparticle curves with the dependence $I_{qp}(V) \propto V^n$ The results for $n = 2$ and $n = \infty$ are shown ($n = 1$ is the RSJ model). The case $n = \infty$ assumes an infinite rise of the quasiparticle current above the gap voltage. Stewart's parameter $k \equiv I_c\phi_0/(2\pi CV_g^2)$ is related to β_c by $\beta_c = k^{-1}(I_cR_n/V_g)^2$, for $n = 2$ and ∞. Finally, the best fit from the digital simulation of the experimental data of How-

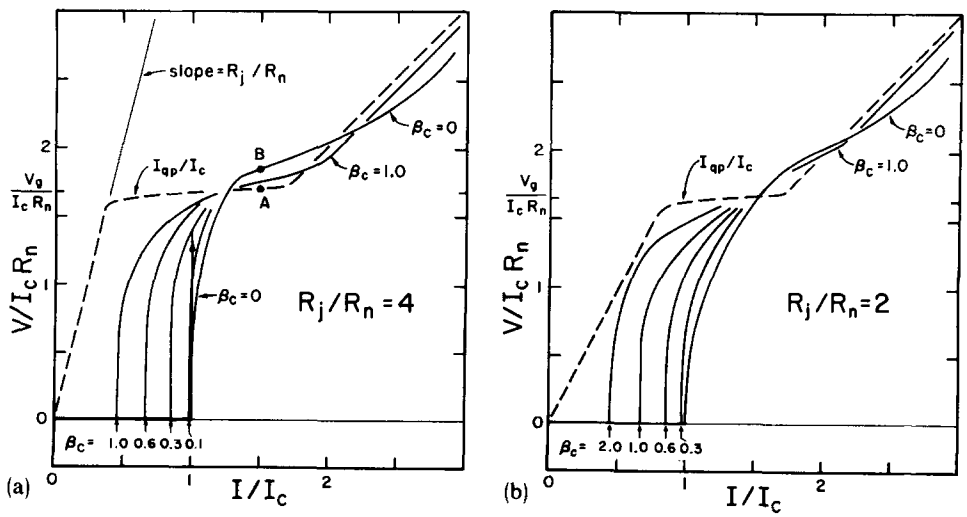

FIG. 3. Normalized current-voltage curves from the analog simulations for two values of sub-gap resistance R_j, (a) $R_j/R_n = 4$, and (b) $R_j/R_n = 2$, and for various β_c values. Quasiparticle current curve I_{qp} is dashed. For clarity, only the curves for $\beta_c = 0$ and 1.0 and the quasiparticle curve are shown for voltages above V_g. Also, the jump to the finite voltage curve when I exceeds I_c is shown only for $\beta_c = 0.3$ in Fig. 3(a). Note crossings of quasiparticle curve and $\beta_c = 0$ curve for $V \gtrsim V_g$. All curves merge at voltages $\gg V_g$.

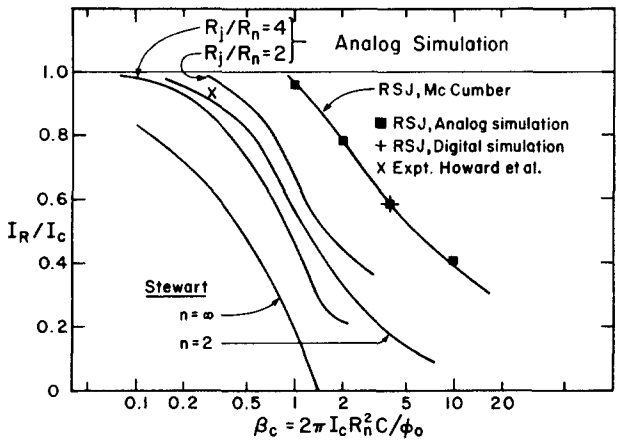

FIG. 4. Normalized return current I_R/I_c as a function of β_c, from the analog simulations for values of $R_j/R_n = 4$, 2, and for the RSJ model; from the digital simulation and from computations of McCumber (Ref. 8) for the RSJ model; and from computations of Stewart (Ref. 5) for a quasiparticle conductance which depends on voltage as V^n, for $n = 2$ and ∞. Also shown is the experimental data point from Ref. 1, with β_c determined from Fig. 2. For the Stewart curves, we have taken $V_g/I_cR_n = 1.7$, as in Fig. 3. (This value is close to that of the experimental results in Refs. 1 and 2.)

ard *et al.* is shown. It lies between the $R_j/R_n = 4$ and $R_j/R_n = 2$ analog simulations, as previously noted.

While the qualitative dependence of I_R/I_c on β_c is similar for the analog simulations and Stewart's computations, there are quantitative differences, and the shapes of the curves also differ. Stewart's model assumes a quasiparticle current *greater* than V/R_n for $V > V_g$. While mathematically tractable, that assumption is not physically reasonable. This is in contrast to the realistic model for I_{qp} employed in our analog simulations. We therefore believe that the analog simulation results will be more accurate in providing a rough assessment of junction quality (i.e., R_j/R_n) if the quasiparticle curve cannot be measured, but β_c can be estimated. These simulation results can also be helpful in determining the amount of external shunt conductance required to eliminate hysteresis.

IV. DISCUSSION

Two features of the simulations are of particular interest: (i) the value of capacitance required for a best fit to the experimentally observed hysteresis, and (ii) the physical origin of the crossing of the quasiparticle and total current curves.

The value of junction capacitance derived, 9×10^{-15} F from the digital simulation and a similar value from the analog simulations, is in fact in good agreement with a value of 7×10^{-15} F which we infer by extrapolating data obtained at IBM by Magerlein.[13] Magerlein studied oxide tunnel barriers formed by rf sputter oxidation[14,15] of Pb-alloy base electrodes with 26.7 at. % Indium. Junctions studied had critical current densities j_c ranging between 100 and 1000 A/cm^2. For $j_c = 10^3$A/cm^2, a specific capacitance, $C_s = 4.4$ μF/cm^2, was measured. C_s depended only weakly on the magnitude of j_c. Extrapolating the expression[13] for C_s, a value of $C_s = 6.5\,\mu$F/cm^2 is obtained for $j_c = 1.2\times10^5$ A/cm^2, appropriate for the junction of Fig. 2. We thus obtain a value of $C = 7\times10^{-15}$ F for a junction of area 10^{-9} cm^2.

While the capacitance value of 7×10^{-15} F obtained above is in reasonable agreement with the value inferred from the digital simulations of 9×10^{-15} F, the agreement must be viewed as qualitative. This is because junction areas, determined by SEM examination, are uncertain by about 20%. Also, the oxide tunnel barriers of the junctions studied in Ref. 1 were formed by thermal oxidation, and not the rf sputter oxidation process. We believe that the general agreement of the capacitance values does suggest that the observed hysteresis is *not* due to extrinsic effects in the electrodes, such as heating or nonequilibrium effects. Such effects in general increase the observed hysteresis.

The second major feature of the simulation results is the crossing of the total current curve and the quasiparticle curve (dashed curve) seen in Figs. 2 and 3. This crossing may at first seem surprising, since it appears that by adding the supercurrent channel in parallel with the quasiparticle channel, *less* current flows at a given voltage in the region of the crossing. In fact, this interpretation is not correct. The curves only show that where the crossing occurs, a larger average voltage is developed when the supercurrent channel is included. We shall demonstrate below that this is a correct and reasonable result of the model considered. It is significant that the crossing feature does not show up in simulations for the RSJ model $[G_{qp}(V) = R^{-1}]$.

To explain the crossing effect, we offer the following reasoning. Consider the simplest case, with $C = 0$, so that only the supercurrent and quasiparticle current contribute to the total current. Recall that the quantity V we must determine is the *time-average* voltage. If we imagine disconnecting the supercurrent channel, so that $I_{qp} = I$, then I_{qp} is a dc current. To be specific, let us take the quasiparticle $I_{qp}(V)$ curve of Fig. 3(a), and set $I = 1.5I_c$. The dc voltage developed across the quasiparticle channel is that at point A, and is approximately equal to the gap voltage $V_A \approx V_g$

If now the supercurrent channel is reconnected in parallel with the quasiparticle channel, the quasiparticle current will oscillate between $I - I_c$ and $I + I_c$, according to Eq. (1). The time-dependent voltage will oscillate along the quasiparticle curve (dashed curve) between $0.5I_c$ and $2.5I_c$. The time-average voltage V must therefore be larger than V_g; it is in fact equal to that at point $B, V_B > V_A$. Thus, for $I \sim 1.5I_c$, connection of the supercurrent channel can *increase* the dc voltage to be above that of the quasiparticle curve. This increased voltage is seen to result simply from averaging the voltage along the *nonlinear* quasiparticle curve.

At higher voltages the nonlinearity of the quasiparticle curve is less important, and the curve for I crosses back over the quasiparticle curve. The voltage averaging along the quasiparticle curve described above still occurs. However, if one stays entirely on the linear section of the I_{qp} curve for $V \gg V_g$, the dc voltage V must be *less* than that of the quasiparticle channel alone. This is because a longer time is spent at lower voltages where the phase increases more slowly [see Eq. (2)]. Thus the two crossing effect evident in Figs. 2 and 3, though apparently counterintuitive, is real and correct for

the model of a *nonlinear* quasiparticle conductance considered. As would be expected from the above arguments, as $R_j \rightarrow R_n$ one approaches the RSJ model[8] and the crossing effect disappears. In the RSJ model, the time-average voltage with the supercurrent channel connected is *always* less than that of the resistive channel alone.

While the crossing seen in the simulation data is real and explicable, it is not seen in the experimental data. Indeed, as seen in Fig. 2, the agreement between the overall shape of the experimental and simulated I-V curves in the vicinity of V_g is only moderate. The experimental curve for the total current I shows a much sharper current increase at the gap voltage than the digitally simulated curves for either 9×10^{-15} F or 50×10^{-15} F. A sharp current rise at $V\approx V_g$ is also seen in other small or low β_c tunnel junctions,[16] and in ideal point contacts.[17] The discrepancy between experiment and simulation therefore appears to be due to a deficiency in the model stated in Eqs. (1) and (2).

A possible improvement in the model used here is to include the frequency dependence of the supercurrent magnitude along with other terms from the microscopic theory.[18] McDonald and co-workers[6] and Zorin and Likharev[6] have used the microscopic theory to calculate junction I-V curves for, respectively, the $T=0$ and the finite temperature cases. The calculated I-V curves do not show the crossing effect. However, the results as a whole show much more structure than is observed experimentally. The electronic analog can be extended to include frequency dependence of I_c,[19] and results of such studies would be of interest.

A second effect not included in the model of Eqs. (1) and (2) is thermal noise. The effects of such noise are expected to be small, because the noise parameter[20] $\Gamma = 2\pi k_B T/I_c\phi_0 = 1.4\times10^{-3}$ is much less than 1. Noise effects might prematurely trigger a return to the zero-voltage state, possibly explaining why the corner of the experimental I-V curve near I_R is sharper than that of the simulation. However, the overall shape of the I-V curve should not be greatly affected, and our qualitative conclusions regarding the crossing effect should still be applicable.

In conclusion, the circuit model used, the resistively shunted junction model with a nonlinear quasiparticle conductance and frequency-independent parameters, [Eqs. (1) and (2)], is not fully sufficient to explain the I-V curves of small, low-capacitance Josephson tunnel junctions. The hysteresis of the experimental I-V curves is reasonably well explained. However, the fact that the simulated curves cross the quasiparticle curve twice, whereas the experimental curve does not cross the quasiparticle curve at all, is not explained. A more refined model, possibly including the frequency dependence of the supercurrent, appears to be required.

A further conclusion may be drawn for those who simulate Josephson computer elements. Most simulations of digital Josephson computer elements[3] employ the same lumped-circuit-element junction model as was used here, with frequency-independent parameters. The fact that the experiments and simulations agree well for the case of previously studied large junctions is in all likelihood due to the effect of the large capacitance, which acts to shunt ac supercurrents and thereby reduce the amplitude of the ac (Josephson) voltage oscillation. As a result, the excursions along the quasiparticle curve are small and nonlinear averaging is of little importance, unlike the case studied in this paper. As junction capacitances are reduced to obtain faster switching speeds and as switching times of a few psec are approached, a more refined model[18] may also be required for the digital circuit simulations.

We wish to thank R. E. Howard and E. L. Hu for informative discussions, and A. Kleinsasser and L. N. Smith for communication of results prior to publication. This work was supported in part by NSF grants ENG 77-10164 and ECS 79-27165. The provision of a sabbatical leave by Bucknell University and the hospitality of the Department of Engineering and Applied Science at Yale University is gratefully acknowledged by one of us (R.W.H.).

[1] R. E. Howard, E. L. Hu, L. D. Jackel, L. A. Fetter, and R. H. Bosworth, Appl. Phys. Lett. **35**, 879 (1979).
[2] E. L. Hu, R. E. Howard, L. D. Jackel, L. A. Fetter, and D. M. Tennant, IEEE Trans. Electron Devices **ED-27**, 2030 (1980).
[3] J. Matisoo, IBM J. Res. Dev. **24**, 113 (1980), and references therein.
[4] W. C. Scott, Appl. Phys. Lett. **17**, 166 (1970); E. Ben Jacob and Y. Imry, J. Appl. Phys. **51**, 4317 (1980); L. N. Smith and D. W. Jillie (unpublished).
[5] W. C. Stewart, J. Appl. Phys. **45**, 452 (1974).
[6] D. G. McDonald, E. G. Johnson, and R. E. Harris, Phys. Rev. B **13**, 1028 (1976); A. B. Zorin and K. K. Likharev, Sov. J. Low Temp. Phys. **3**, 70 (1977).
[7] D. G. McDonald, R. L. Peterson, and B. K. Bender, J. Appl. Phys. **48**, 5366 (1977). In this work a value of the Josephson penetration depth $\lambda_J = 0.8\,\mu$m has been calculated for Pb-alloy junctions with $j_c = 1.6\times10^5$ A/cm^2, similar to those of Refs. 1 and 2.
[8] W. C. Stewart, Appl. Phys. Lett. **12**, 277 (1968); D. E. McCumber, J. Appl. Phys. **39**, 3113 (1968).
[9] J. T. C. Yeh and R. A Buhrman, Appl. Phys. Lett. **31**, 362 (1977).
[10] See, for example, D. D. McCracken and W. S. Dorn, *Numerical Methods and Fortran Programming* (Wiley, New York, 1964).
[11] R. W. Henry, D. E. Prober, and A. Davidson, Am. J. Phys. **49** (1981) (to be published). R. W. Henry and D. E. Prober, Rev. Sci. Instrum. **52**, June 1981 (to be published). Full circuit and construction details for the electronic analog are given in these articles. The former article treats basic aspects of the single-junction analog. That analog uses a mixter-type sinθ circuit, as suggested by C. K. Bak and N. F. Pederson, Appl. Phys. Lett. **22**, 149 (1973). The mixer-type sinθ circuit gives less exact agreement with the computed RSJ results of Ref. 8 for finite capacitance than the sample-and-hold sinθ circuit employed in the latter article and in this paper.
[12] J. H. Magerlein, Rev. Sci. Instrum. **49**, 486 (1978); D. B. Tuckerman, Rev. Sci. Instrum. **49**, 835 (1978); A. Yagi and I. Kurosawa, Rev. Sci. Instrum. **51**, 41 (1980).
[13] J. H. Magerlein, IEEE Trans. Magn. **MAG-17**, 286 (1981).
[14] J. H. Greiner, J. Appl. Phys. **42**, 5151 (1971).
[15] John M. Baker, C. J. Kircher, and J. W. Matthews, IBM J. Res. Dev. **24**, 223 (1980).
[16] J. Niemeyer and V. Kose, Appl. Phys. Lett. **29**, 380 (1976); E. L. Hu, L. D. Jackel, R. W. Epworth, and L. A. Fetter, IEEE Trans. Magn. **MAG-15**, 585 (1979); A. W. Kleinsasser and R. A. Buhrman, Appl. Phys. Lett. **37**, 941 (1980).
[17] D. A. Weitz, W. J. Skocpol, and M. Tinkham, J. Appl. Phys. **49**, 4873 (1978).
[18] E. Riedel, Z. Naturforschung **19a**, 1634 (1964); N. R. Werthamer, Phys. Rev. **147**, 255 (1966). A recent formulation of the theory by R. E. Harris, J. Appl. Phys. **48**, 5188 (1977), may be more directly applied for calculation of time-domain response. However, realistic quasiparticle curves must be included, since the subgap quasiparticle conductance affects the shape of the I-V curves, as we have shown in the present work.
[19] D. G. Jablonski and J. R. Waldram, SQUID'80, H. D. Hahlbohm and H. Lübbig (deGruyter, New York, 1980), p. 115.
[20] V. Ambegaokar and B. I. Halperin, Phys. Rev. Lett. **22**, 1364 (1969).